Journal of Cerebral Blood Flow and Metabolism
16:427–438 © 1996 The International Society of Cerebral Blood Flow and Metabolism
Published by Lippincott–Raven Publishers, Philadelphia

^{1}H NMR Studies of Glucose Transport in the Human Brain

Rolf Gruetter, †Edward J. Novotny, †Susan D. Boulware, *Douglas L. Rothman, and Robert G. Shulman

*Departments of Molecular Biophysics and Biochemistry, *Internal Medicine, and †Pediatrics, Yale University and School of Medicine, New Haven, Connecticut, U.S.A.*

Summary: The difference between ^{1}H nuclear magnetic resonance (NMR) spectra obtained from the human brain during euglycemia and during hyperglycemia is depicted as well-resolved glucose peaks. The time course of these brain glucose changes during a rapid increase in plasma glucose was measured in four healthy subjects, aged 18–22 years, in five studies. Results demonstrated a significant lag in the rise of glucose with respect to plasma glucose. The fit of the integrated symmetric Michaelis–Menten model to the time course of *relative* glucose *signals* yielded an estimated plasma glucose concentration for half maximal transport, K_t, of 4.8 ± 2.4 m*M* (mean ± SD), a maximal transport rate, T_{max}, of 0.80 ± 0.45 μmol g^{-1} min^{-1}, and a cerebral metabolic glucose consumption rate $(CMR)_{glc}$ of 0.32 ± 0.16 μmol g^{-1} min^{-1}. Assuming cerebral glucose concentration to be 1.0 μmol/g at euglycemia as measured by ^{13}C NMR, the fit of the same model to the time course of brain glucose *concentrations* resulted in K_t = 3.9 ± 0.82 m*M*, T_{max} = 1.16 ± 0.29 μmol g^{-1} min^{-1}, and CMR_{glc} = 0.35 ± 0.10 μmol g^{-1} min^{-1}. In both cases, the resulting time course equaled that predicted from the determination of the steady-state glucose concentration by ^{13}C NMR spectroscopy within the experimental scatter. The agreement between the two methods of determining transport kinetics suggests that glucose is distributed throughout the entire aqueous phase of the human brain, implying substantial intracellular concentration. **Key Words:** Glucose transport—Blood-brain barrier—Magnetic resonance spectroscopy—Human—Michaelis–Menten.

Human brain function depends upon a continuous supply of glucose from the blood. The specific glucose transport mechanism from the blood has been shown to be of the insulin-independent facilitated diffusion type with saturation kinetics (Crone, 1965; for reviews see e.g. Pardridge 1983; Lund-Andersen, 1979; Pelligrino et al., 1992; Gjedde, 1992) and is mediated by transporter molecules (Mueckler et al., 1985; Kalaria et al., 1988), mostly GLUT-1 (Pardridge et al., 1990) in the capillary endothelial cells, referred to as the blood–brain barrier (BBB). Free glucose is measurable in *animal* brain (Gjedde and Diemer, 1983; Holden et al., 1991; Mason et al., 1992). Under physiological conditions, free glucose is measurable in the *human* brain (Gruetter et al., 1992*a*) providing direct evidence that transport rates are in excess of the metabolic rate. Glucose transport may, however, become rate-limiting to the metabolic rate in a variety of situations, such as hypoglycemia, seizures (Siesjö, 1978), molecular defects of glucose transporter (DeVivo et al., 1991), hypoxic–ischemic encephalopathy, and Alzheimer's disease (Kalaria and Harik, 1989). Quantitative measurements of glucose transport using radioactive tracers have been difficult to interpret in humans (Brooks et al., 1986; Feinendegen et al., 1986; Gutniak et al., 1990; Blomqvist et al., 1991), because the contribution of radiolabeled glucose or glucose analogs to the time course of measured tissue radioactivity needs to be deconvoluted from the accumulation of radioactivity in metabolic intermediates or products. It is well established that the brain glucose concentration is a crit-

Received October 19, 1994; final revision received August 21, 1995; accepted August 21, 1995.

Address correspondence and reprint requests to Dr. Rolf Gruetter at Department of Radiology, University of Minnesota Medical School, Clinical Research Center and Center for Magnetic Resonance Research, 385 East River Road, Minneapolis, MN 55455, U.S.A.

Abbreviations used: BBB, blood-brain barrier; CMR_{glc}, cerebral metabolic rate of glucose; NMR, nuclear magnetic resonance; PET, positron emission tomography; TE, echo time; TI, inversion time; TR, repetition time.

ical parameter in the analysis of results from experiments using radiolabeled glucose or glucose analogs (Gjedde and Diemer, 1983; Gjedde 1982; Holden et al., 1991; Sokoloff, 1984).

A study performed in this laboratory by noninvasive ^{13}C nuclear magnetic resonance (NMR) determined the brain glucose concentration in humans to be 1.0 ± 0.1 μmol/ml brain volume at euglycemia (Gruetter et al., 1992*a*). The kinetic parameters of glucose transport were determined by measuring the steady-state brain glucose concentration as a function of plasma glucose and by fitting the data to the symmetric Michaelis–Menten model of glucose transport (Lund-Andersen, 1979; Gjedde and Christensen, 1984). This model assumes that the blood-brain barrier is rate-limiting for glucose transport into the entire brain with transport from extracellular to intracellular space being relatively rapid.

A limitation of determining kinetic constants from the relationship between brain and plasma glucose concentrations is the dependence upon the assumption that the rate-limiting step for glucose transport into the brain cells is at the BBB. Alternatively, the rate-limiting step could be at the cell membrane, and the glucose measured by ^{13}C NMR is entirely within the extracellular space at near-equilibrium with plasma glucose. In this case, intracellular glucose would be zero and transport at the cell membranes would be rate-limiting for metabolism. To test these possibilities, we derived brain glucose transport kinetics from the time course of the change in brain glucose measured by the more sensitive ^{1}H NMR difference spectroscopy after a rapid increase in plasma glucose concentration. The observed time course of changes in brain glucose concentration in the occipital lobe was compared directly to the time course predicted from the kinetic constants derived from steady-state measurements of brain glucose concentrations (Gruetter et al., 1992*a*). Included are also some quantitative estimates of the contribution of the glucose signal to the ^{1}H NMR signal at euglycemia. A preliminary report has appeared previously (Novotny et al., 1992).

METHODS

All experiments were carried out on a 2.1 Tesla whole-body magnet (Oxford Magnet Technology, Oxford, England) with an extensively modified Biospec spectrometer (Bruker-ORS, Billerica, MA, U.S.A.) equipped with an active-shielded gradient set (Oxford) of 72 cm clear diameter. Subjects were positioned in the supine position on an elliptic 6 × 7 cm diameter surface coil. Positioning was based on MR inversion recovery images—inversion time (TI) = 800 ms, echo time (TE) = 10 ms, repetition time (TR) = 2.5 s)—obtained as gradient echoes in sagittal and transverse planes. Localized automatic shimming was performed on all first- and second-order shim coils using FASTMAP (Gruetter, 1993). A volume of 36 ml was localized in the occipital lobe of the brain using the pulse sequence described previously (Gruetter et al., 1992*b*), with some modifications: Three-dimensional localization was obtained with ISIS (Ordidge et al., 1986) in conjunction with 5.5 ms phase-swept hyperbolic secant pulses (Silver et al., 1984; Baum et al., 1985) with $\mu = 8$ resulting in 4 kHz bandwidth. Outer volume suppression using 9-ms noise pulses (Connelly et al., 1988) was applied in the two planes perpendicular to the coil. The signal was detected as a spin echo (TE = 16 ms) generated by a sinc pulse defined over $\pm 5\pi$ exciting a slice parallel to the surface coil plane in conjunction with a semiselective binomial refocusing $\theta_x - \tau - \theta_{-x}$ pulse, where τ was set to 5 ms. Use of the semiselective refocusing pulse separated the spatial and frequency selectivities and generated a positive amplitude throughout the spectrum (Blondet et al., 1987). A θ/3 pulse prior to the localization sequence was used to reduce signals from high B_1 flux regions (Shaka and Freeman, 1985). Unwanted transverse coherences were dephased by gradient pulses and surface gradient spoiler pulses (Chen and Ackerman, 1989) throughout the sequence. Longitudinal magnetization was minimized after the data acquisition period of 256 ms by applying a 90° composite pulse (Levitt and Ernst, 1983), i.e., $(\theta/2)_x(\theta/2)_y(\theta/2)_x(\theta/2)_{-y}$. Water suppression was achieved by the semiselective refocusing pulse and by low power presaturation (<0.2 Watts total) during the recovery delay, which was applied with a second low-power amplifier through a directional coupler. In order to correct for field drift during blood sampling, spectra were collected in 3-min blocks (64 scans, 2.5 s repetition time). Difference spectra were obtained by extensive zero filling and corrected for frequency shifts only. Constant phase corrections were maintained throughout each study. Difference spectra were processed with Lorentzian-to-Gaussian conversion (Gaussian factor = 0.15, Lorentzián = −5Hz) plus baseline correction between 2.5 and 4.5 ppm and were expressed in % of the maximum increase, defined by the mean of the last four measurement points.

Catheters were placed into the left antecubital vein for the glucose infusion and the right upper extremity was catheterized to obtain blood samples. To aid with sampling of arterialized blood, preheated saline bags were placed at the elbow and at the wrist. Plasma glucose concentrations were measured every 5 min in a Beckman glucose analyzer (Beckman, Fullerton, CA, U.S.A.) using the glucose oxidase technique. A variable priming infusion of glucose, dextrose, 20% (wt/vol) was begun at t = 0 min so that the plasma glucose concentration was raised acutely and maintained ~10 m*M* above baseline for 60 min according to previously described procedures (De Fronzo et al., 1979; Shulman et al., 1990). A total of five studies were performed in four subjects (18–22 years). Full written informed consent was obtained prior to each study, which was approved by the Yale Human Investigations Committee. Sensory stimulation was minimized by having subjects wear eye patches and ear plugs.

Kinetic analysis of time courses

To analyze the time course of incremental brain glucose changes, we used the integrated symmetric Michaelis–Menten model of glucose transport (Lund-Andersen, 1979; Carruthers, 1990), shown in Fig. 1A.

This model assumes identical *apparent* Michaelis–Menten kinetics for both transport in, T_{in}, and out, T_{out}, of the brain. The model is entirely characterized by the *apparent* half-saturation constant K_t (m*M* plasma glucose concentration), the *apparent* maximal transport rate, T_{max} (μmol g^{-1} min^{-1}), the glucose consumption rate, CMR_{glc} (μmol g^{-1} min^{-1}), and the distribution volume of glucose, V_d = 0.77 ml/g (Lund-Andersen, 1979; Gjedde and Diemer, 1983). Using the kinetic constants of this model, the differential equation

$$\frac{dG_{brain}(t)}{dt} = T_{max}\frac{G_{plasma}(t)}{K_t + G_{plasma}(t)} - T_{max}\frac{G_{brain}(t)}{V_dK_t + G_{brain}(t)} - CMR_{glc} \quad (1)$$

describes the change in brain glucose $G_{brain}(t)$ (μmol/g) as a function of changes in plasma glucose $G_{plasma}(t)$ (m*M*). The time-independent form of this equation (Eq. 3) has been used in a number of studies to determine glucose transport kinetics from steady-state glucose measurements in animal (e.g., Gjedde and Christensen, 1984; and refs therein; Holden et al., 1990; Mason et al., 1992) and human brain (Gruetter et al., 1992*a*).

T_{max} represents the rate of product formation when the enzyme substrate complex concentration equals the total enzyme concentration, E_{tot}. In the present model, T_{max} is, therefore, by definition a constant with respect to G_{plasma}. Conversely, K_t is the Michaelis–Menten constant, i.e., the plasma glucose concentration at which the transport rate is half-maximal. Note that this model assumes that the rate of product formation (transport of glucose into the brain) is not significantly product inhibited. CMR_{glc} is assumed to be constant since hexokinase is heavily saturated under the conditions of this study. An alteration of CMR_{glc} through, e.g., a change in V_{max}, is unlikely based on the evidence of studies showing that net glucose uptake at hyperglycemia is constant (e.g., Pappenheimer and Setchell, 1972). In addition, evidence from studies using ^{13}C-labeled glucose and NMR from this brain region measured under identical experimental conditions (Gruetter et al., 1994; Mason et al., 1995) show that at glycemia similar to that of this study, the measured CMR_{glc} agrees with values obtained by other methods at euglycemia.

Equation 1 is justified from the Michaelis–Menten condition, which requires the rate of the enzyme-substrate complex formation and breakdown to be fast compared to the rate of product formation (Mahler and Cordes, 1971). A rise in plasma glucose from 5 to 15 m*M* in 10 min corresponds to change from 50 to 75% transporter saturation (assuming a K_t of ~5 m*M*), i.e., a 2.5%/min rise, which is much slower than the 0.1 s of equilibration re-

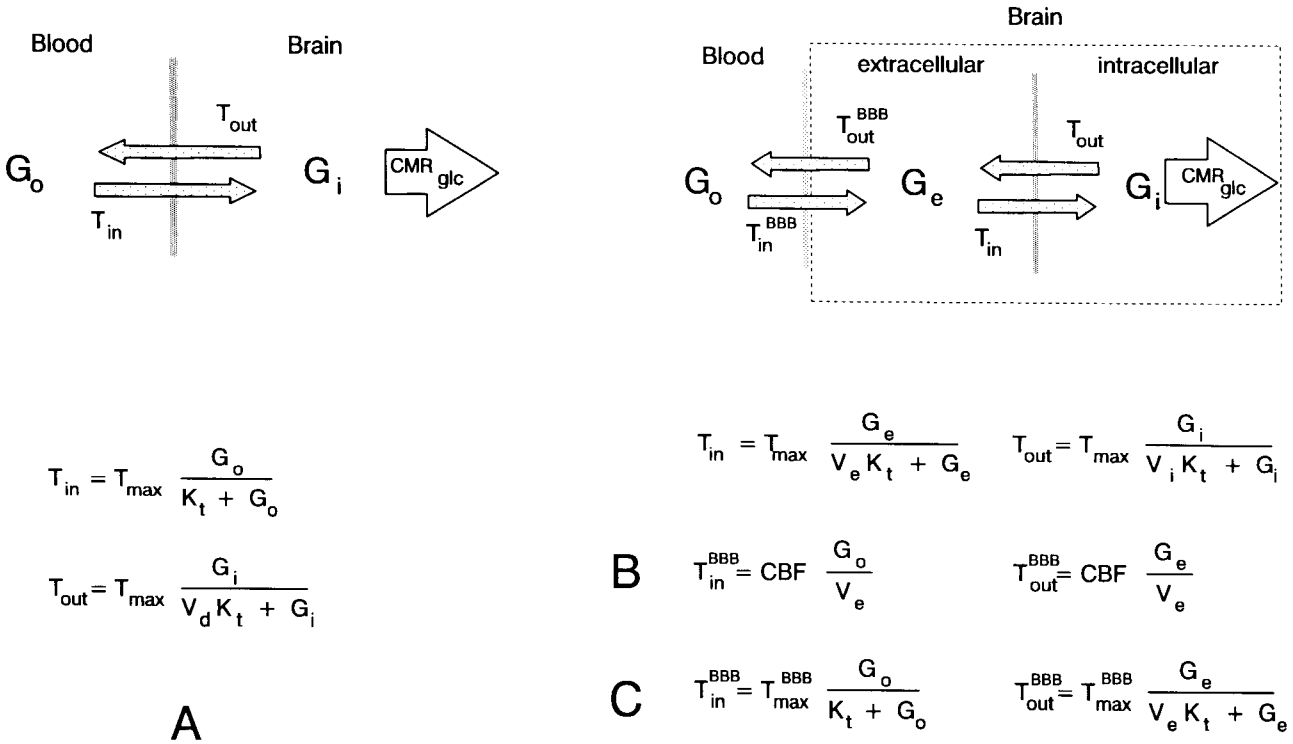

FIG. 1. Models of glucose transport in the human brain. **A:** This model assumes that transport across the blood-brain barrier (BBB) is rate-limiting and that equilibration within the brain is fast, resulting in a single kinetic pool within the brain. Influx, T_{in}, and efflux, T_{out}, across the BBB are characterized by Michaelis-Menten kinetics with identical kinetic constants, T_{max} and K_t. Physical distribution volume of glucose is the entire aqueous phase of water, V_d = 0.77 ml/g (Eq. 1). **B:** In this model, intracellular glucose, G_i, is assumed to be 0 and extracellular glucose, G_e, in free exchange with plasma glucose, G_o, using Fick's principle with an average CBF of 0.5 ml/g^{-1} min^{-1} (Eq. 6). **C:** In this model, it was assumed that all of the brain glucose is in extracellular space (V_e = 0.2 ml/g), but that glucose transport across the BBB is described by Michaelis–Menten kinetics using Eq. 1 with V_d = V_e = 0.2 ml/g. In this case, T_{max}/CMR_{glc} is >25 given the concentrations reported by Gruetter et al., (1992a). V_e was set to 0.2 ml/g and $V_i = V_d - V_e$

ported for endothelial cells (Gjedde and Christensen, 1984) suggesting that the rate of glucose-transporter complex formation is several orders of magnitude faster than the rate of plasma glucose concentration change achievable in humans.

Since changes in glucose concentration were measured, Eq. 1 was rewritten as

$$\frac{d\Delta G_{brain}(t)}{dt} = T_{max}\frac{G_{plasma}(t)}{K_t + G_{plasma}(t)} - T_{max}\frac{(\Delta G_{brain}(t) + G^{(i)}_{brain})}{V_d K_t + (\Delta G_{brain}(t) + G^{(i)}_{brain})} - CMR_{glc} \quad (2)$$

Differential brain glucose is given by $\Delta G_{brain}(t) = G_{brain}(t) - G^{(i)}_{brain}$ and the initial steady-state brain glucose concentration $G^{(i)}_{brain}$ is given by Eq. 3, the steady-state formulation of Eq. 1 at the initial plasma glucose concentration $G^{(i)}_{plasma}$:

$$G^{(i)}_{brain} = V_d K_t \frac{\left(\frac{T_{max}}{CMR_{glc}} - 1\right)\frac{G^{(i)}_{plasma}}{K_t} - 1}{\frac{T_{max}}{CMR_{glc}} + \frac{G^{(i)}_{plasma}}{K_t} + 1} \quad (3)$$

For numerical simulations, Eq. 2 was solved to give $\Delta G_{brain}(t)$ using nonlinear methods with $G_{plasma}(t)$ derived from the linear interpolation of the measured plasma glucose concentrations. The term $V_{blood} \times \Delta G_{plasma}(t)$ was added to give the change in total observed glucose signal $\Delta G_{obs}(t)$, i.e.,

$$\Delta G_{obs}(t) = \Delta G_{brain}(t) + \Delta G_{plasma}(t) \times V_{blood} \quad (4)$$

to account for a small potential contribution of plasma glucose to the signal. V_{blood} was set to 0.035 ml/g based on position emission tomography (PET) and other measurements of blood volume in human gray matter (Marchal et al., 1992; Hino et al., 1992; Sabatini et al., 1991). The average of the last four time points of $\Delta G_{obs}(t)$, i.e., $G^{(f)}_{obs}$ was used to scale $\Delta G_{obs}(t)$ to 100%, giving $G^{*}_{norm}(t)$ (Eq. 5).

$$G^{*}_{norm}(t) = 100\frac{\Delta G_{obs}(t)}{G^{(f)}_{obs} - G^{(i)}_{obs}} \quad (5)$$

Differential equations were solved using the Bulirsch-Stoer algorithm (Press et al., 1989). All numerical solutions were performed on a 16 MHz Zenith 386SX desktop computer equipped with a 387SX coprocessor using Turbo Pascal 6.0 Professional (Borland). In order to maintain computational efficiency, $n \leq 3$ variables fitted to the data.

In order to further evaluate the assumptions of the symmetric Michaelis–Menten model of glucose transport, e.g., large physical distribution space and the rate-limiting step for transport at the BBB, three models were tested as described in Fig. 1; the numerical analysis performed is described below:

Model A: Symmetric Michaelis–Menten model (Fig. 1A). This model assumes that transport across the BBB is rate-limiting and equilibration within the brain is fast, resulting in a single kinetic pool within the brain. Influx, T_{in}, and efflux, T_{out}, across the BBB are characterized by Michaelis–Menten kinetics with identical kinetic constants, T_{max} and K_t. Physical distribution volume of glucose is the entire aqueous phase of water, $V_d = 0.77$ ml/g (Eq. 1). Fitting of the resulting Eq. 5 to the experimental time course was performed by minimizing the sum of squared residuals over a grid search of $T_{max} = 0.4..1.6$ μmol g^{-1} min^{-1}, $CMR_{glc} = 0.20–0.50$ μmol g^{-1} min^{-1}, and $K_t = 1.0..8.0$ m*M*. This fit was then compared with the values determined by the ^{13}CMR experiments.

In a different analysis, we used the kinetic constants from the ^{13}C NMR measurements (Gruetter et al., 1992*a*) to determine the initial and final glucose concentrations based on plasma glucose concentration. The time course of brain glucose $G_{obs}(t)$ was then fitted based on Eq. 4 in order to assess whether this additional information improved the precision of T_{max}, and K_t, andCMR_{glc} determination.

Model B: Fast exchange between plasma and extracellular glucose. An alternative explanation for the ^{13}C NMR measurements is that the observed brain glucose enters the brain by rapid free diffusion only into the extracellular space. In this model, intracellular glucose G_i is assumed to be zero and extracellular glucose G_e in free exchange with plasma glucose, G_o, using Fick's principle, shown in Fig. 1B, by solving

$$\frac{dG_{brain}(t)}{dt} = \frac{CBF}{V_{ecf}}(V_{ecf}G_{plasma}(t) - G_{brain}(t)) - CMR_{glc} \quad (6)$$

instead of Eq. 1 and scaled analogously. As shown in Results, with an average CBF = 0.5 ml/g^{-1} min^{-1} and an extracellular volume of 0.20 ml/g, the resulting time course of glucose in extracellular space follows closely that in plasma with a lag <1 min.

Model C: Michaelis–Menten kinetics for fast exchange at the BBB. In this model, it is assumed that all of the brain glucose is in extracellular space ($V_e = 0.2$ ml/g, $G_i = 0$), but that glucose transport across the BBB is described by Michaelis–Menten kinetics using Eq. 1 with $V_d = V_e = 0.2$ ml/g as indicated in Fig. 1C, assuming $G_i = 0$, i.e., $T_{out} = 0$, $T_{in} = CMR_{glc}$. The previous quantification by ^{13}C NMR is, in that case, consistent with a lower limit for T_{max}/CMR_{glc} of 25, as derived by fitting Eq. 3 to the measured steady-state glucose concentrations given in Gruetter et al. (1993). In these simulations $T_{max}/CMR_{glc} = 25$ was, therefore, assumed, resulting in a lag to plasma glucose that was similar to that in model B, i.e., 1 min.

Calculation of the distribution space of glucose. In a fourth set of simulations, we fitted V_d in Eq. 1, instead of CMR_{glc}, which was set to 0.35 μmol g^{-1} min^{-1}, based on previous measurements in the occipito-parietal region by radioisotope methods (Heiss et al., 1984; Tyler et al., 1988) and by ^{13}C NMR (Gruetter et al., 1994; Mason et al., 1995). For this purpose, the differential Eq. 4 was fitted to the change in brain glucose expressed in μmol/g, as described in model A. The minimization of χ^2 was performed using the direction set (Powell) method (Press et al., 1989).

RESULTS

Assignment of in vivo glucose resonances

Measurement of the brain glucose concentrations by localized ^{13}C NMR had the advantage of being

a direct quantitative measurement of well-resolved peaks, albeit with relatively low spatial and temporal resolution. In another study, we showed that ^1H NMR difference spectroscopy can be used to measure changes in brain glucose content after a rapid increase in plasma glucose (Gruetter et al., 1991; Gruetter et al., 1992b; Gruetter et al., 1993) with much higher sensitivity than ^{13}C NMR.

Figure 2A shows regions of short-echo ^1H NMR spectra (TE = 16 ms) obtained at euglycemia (4.8 m*M*) and hyperglycemia (18 m*M*) during a study. The dominant resonance was that of H_2O at 4.72 ppm. At hyperglycemia, significant signal increases were seen at 5.23, 3.81, and 3.44 ppm in the spectra, as indicated by the dotted vertical lines. The corresponding difference spectrum is shown in Fig. 2B and is compared to a spectrum of a phantom, containing equimolar creatine and glucose [~150 m*M* phosphate buffer (pH 7.1), 2 m*M* NaN_3, 10 m*M* acetate, T 37°C]. The solution spectrum was linebroadened to match in vivo creatine linewidths. Chemical shifts and relative amplitudes in the in vivo difference spectrum (Fig. 2B) corresponded to those of glucose in the linebroadened solution spectra.

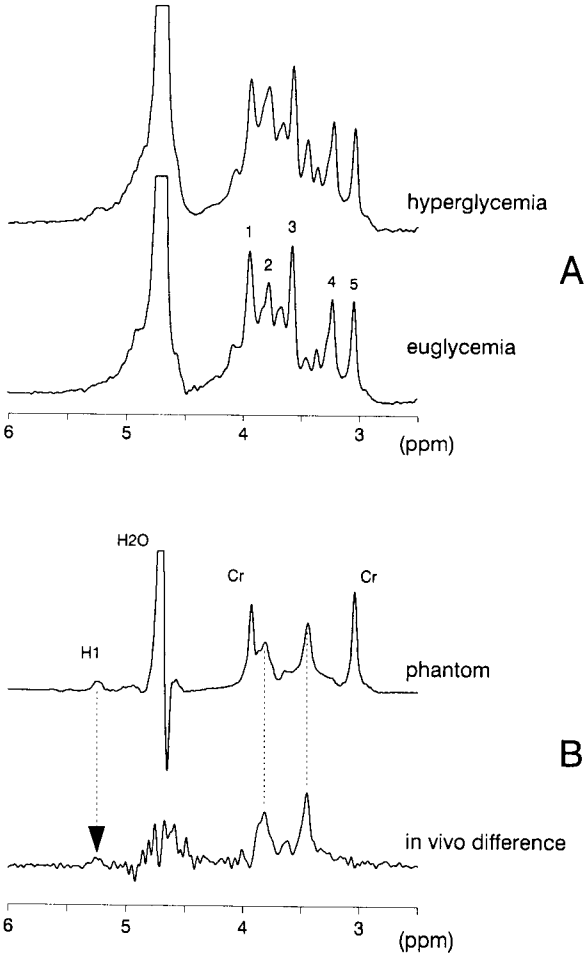

FIG. 2. ^1H MR spectra (TE = 16 ms) acquired before and during glucose infusion. **A:** The spectra represent 15 min summations prior to glucose infusion (bottom) where the plasma glucose concentration was 5 m*M*, and 15 min during the infusion (top) at 17 m*M* plasma glucose. Spectra were obtained by straight Fourier transformation of the zero-filled FID without any apodization using a zero-order phase correction only. **B:** Corresponding in vivo difference spectrum (bottom). The difference spectrum was obtained by correcting for field drift only, i.e., by shifting the zero-filled spectra digitally. The solution spectrum (top) was obtained under identical experimental conditions from a preheated 2 L bottle placed on the surface coil containing glucose and equimolar creatine, ~150 m*M* phosphate buffer (pH 7.1, 37°C), and 10 m*M* acetate plus 2 m*M* NaN_3. The solution spectrum was line broadened until the line width of acetate matched that of singlets (Cr, NAA) in the in vivo spectra. Assignments (major constituents): 1: (phospho)creatine CH_2, 2: αH protons of amino acids, 3: *myo*-inositol, 4: choline and other trimethylamine resonances, 5: (phospho)creatine CH_3. *N*-acetylaspartate at 2.02 ppm (not shown) was used as chemical shift reference.

Assessment of spectral overlap

Although measurement of total brain glucose levels by ^1H NMR has been attempted without taking into account contributions of other compounds to the NMR signal (Gyngell et al., 1991; Merboldt et al., 1992; Kreis and Ross, 1992), direct measurement is difficult due to overlap with resonances of other brain metabolites, in contrast to difference spectra, which are well resolved (Gruetter et al., 1992b).

While increments of glucose concentrations are measurable from the difference spectra, the direct quantification of glucose by ^1H NMR spectroscopy is hampered by the close proximity of the water signal and by overlap with resonances from taurine, inositol, glutamate, and glutamine, all of which are more concentrated than is glucose in the brain (Petroff et al., 1989). At 3.44 ppm overlap from taurine and *myo*-inositol can be expected at 2.1 Tesla based on chemical shifts, coupling patterns, and concentrations in human brain. The average increase of plasma glucose, from 5 to 17 m*M*, doubled the amplitude at 3.44 ppm. From the ^{13}C NMR measurement of brain glucose (Gruetter et al., 1992*a*), this corresponds to a 2.8 μmol/ml brain volume change in brain glucose concentration, suggesting that ~⅓ of the amplitude in the euglycemic spectrum is due to glucose.

To estimate the contribution of *myo*-inositol at the 3.44 ppm glucose resonance, the *myo*-inositol solution spectrum was subtracted from the in vivo spectrum (Fig. 3). The subtraction was performed interactively using standard spectrometer software (DISR88) and minimized the amplitude at 3.57 ppm to 7 ± 5% of its original value (mean ± SD). An analysis of five 15-min spectra yielded a concomi-

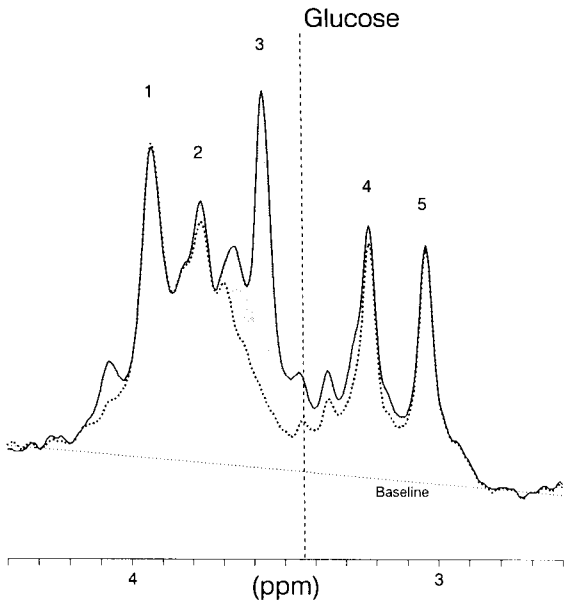

FIG. 3. Influence of *myo*-inositol on glucose amplitude at 3.44 ppm at short echo-time TE = 16 ms. Shown is the in vivo spectrum (solid line) and the same spectrum with the line-broadened solution spectrum of *myo*-inositol subtracted (dotted line). The shaded area indicates the contribution of *myo*-inositol to the in vivo spectrum. The vertical dashed line indicates the position of glucose at 3.44 ppm. For peak assignments, see Fig. 2.

tant 55 ± 3% (mean ± SD) decrease in amplitude at the glucose position (3.44 ppm). Note that the shape and area of the trimethylamine peak (peak 4 in Fig. 3) is affected by the contributions of *myo*-inositol, reducing an apparent asymmetry. That contribution is from the triplet of H2 of *myo*-inositol at this field strength.

Elevated ^{1}H NMR glucose resonances in patients with hyperglycemia due to diabetes have been reported previously at this chemical shift (Michaelis et al., 1991). However, poor correlation between glycemia and the signal area at 3.44 ppm was found in the study by Kreis and Ross, (1992). Our attempts to further resolve that spectral region (Fig. 3) indicate that a substantial nonglucose signal is present at 3.44 ppm, stemming predominantly from *myo*-inositol, as confirmed by measuring at echo TEs of 16–160 ms (not shown). The majority, i.e., half of the amplitude at euglycemia is from *myo*-inositol and we estimate, based on the predicted value from ^{13}C NMR, that just one-third of the amplitude is from glucose. A tight correlation between steady-state brain glucose concentration and plasma glucose, however, was observed by ^{13}C NMR in normal and diabetic humans (Novotny et al., 1993). The low degree of correlation between plasma glucose and brain glucose signal in ^{1}H NMR spectra of diabetics reported by others hence may have been due to variations in overlapping *myo*-inositol resonances, levels of which have been shown to change in diabetes (Stewart et al., 1967).

Time course of observed brain glucose concentration during infusion

During the intravenous infusions of glucose, difference spectra were obtained at 4–5 min intervals. Figure 4 shows the time course of *difference* spectra from one study. Both the 3.81 and 3.44 ppm glucose peaks are clearly discernible and well resolved from other background resonances, which are completely subtracted over the entire time period. The pulse sequence and shimming used resulted in a highly stable baseline, water suppression, and a frequency selective amplitude. To obtain the time courses for kinetic analysis, spectra were processed

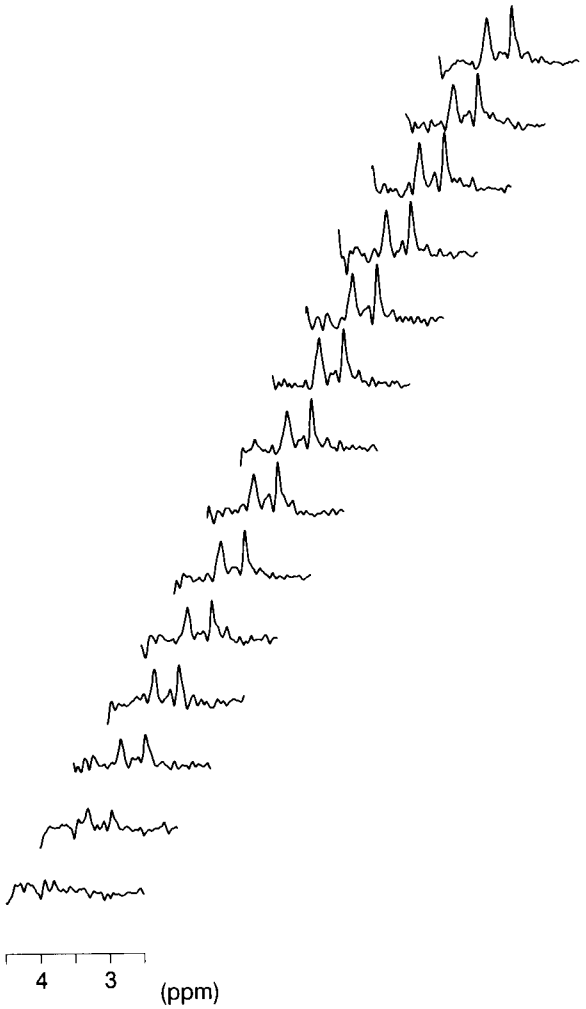

FIG. 4. Time course of the change in the glucose signal. Stack plot of the upfield glucose resonances in the in vivo difference spectra. A time resolution of 3–4 min was achieved by subtracting an averaged spectrum obtained at euglycemia from each 3-min spectrum obtained during infusion. Processing consisted of Gaussian multiplication and baseline correction from 2.5 to 4.5 ppm.

with Gaussian multiplication and the amplitude was measured at 3.44 ppm in baseline-corrected difference spectra.

Both parts of Fig. 5 show the time course of plasma and brain glucose of Fig. 4. At t = 0 min, a steep increase in plasma glucose (triangles) was achieved by the variable priming infusion of glucose. The solid squares represent the difference amplitude of glucose as measured by ^1H NMR and show a clear lag of brain glucose behind plasma glucose, i.e., 4.0 ± 1.0 min (mean ± SEM) at 50% of the maximum increase ($p < 0.05$). The solid line in Fig. 5A is the time course calculated from the parameters of the symmetric Michaelis–Menten model of glucose transport measured by ^{13}C NMR (Gruetter et al., 1992*a*), assuming a cerebral blood volume of 0.035 ml/g (Eq. 5). The dashed line (which almost completely overlaps the solid line) is the best fit of the model to the time course of this study. In Fig. 5B, the solid line is the expected time course assuming brain glucose in extracellular space (~20% of brain volume) to be in free exchange with blood. The solid line parallels the change in plasma glucose, which is inconsistent with the experimental observation. The dashed line is the time course derived by assuming Michaelis–Menten kinetics at the BBB with all glucose being in extracellular space, for which T_{max}/CMR_{glc} must be >25, based on the previous quantification of brain glucose (see methods and below).

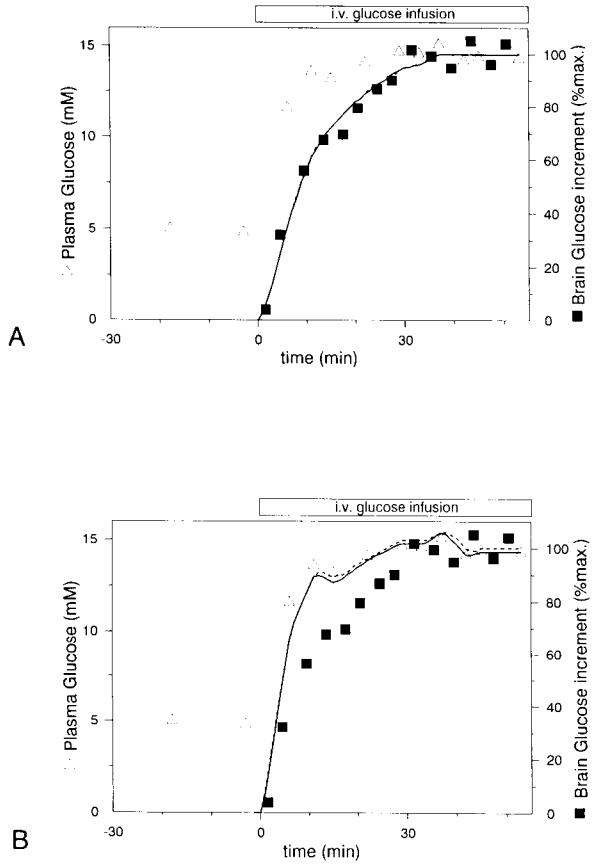

FIG. 5. Time course of the peaks in Fig. 4. The amplitude of the downfield glucose peak at 3.44 ppm (solid squares) was measured and expressed in % of the maximum increase, defined as the average of the last four points. Plasma glucose concentrations (triangles) were measured in a Beckman glucose analyzer. **A:** Shown are incremental time courses of brain glucose predicted from Gruetter et al., 1992*a*, i.e., by quantifying cerebral glucose at steady-state (solid line) and by fitting to this study (dashed line). **B:** The solid line parallels *plasma* glucose changes and was derived analogously using Fick's principle (kinetic model B) and an average CBF of 0.5 ml/g min (Eq. 5). The dashed line was derived assuming G_i = 0 and saturation kinetics at the blood-brain barrier according to Fig. 1**C** and text (model C).

Assessment of transport kinetics

The kinetic analysis distinguished several possibilities, as described in methods:

Model A: Symmetric Michaelis–Menten model. Based on the aforementioned difficulties in measuring steady-state glucose concentrations directly by ^1H NMR, we used relative glucose signal increases to derive experimental fits of Eq. 5 to obtain kinetic constants (Fig. 5). A plasma glucose concentration of half-maximal transport K_t = 4.8 ± 2.4 m*M* (mean ± SD), a maximal transport rate of T_{max} = 0.80 ± 0.45 μmol g^{-1} min^{-1}, and a glucose consumption rate of CMR_{glc} = 0.32 ± 0.16 μmol g^{-1} min^{-1} were obtained from the fit of Eq. 5 to the five studies (row 1 in Table 1).

Since we established, in a previous study, that cerebral glucose concentration is 1.0 ± 0.1 μmol/g (mean ± SEM) at euglycemia, we also solved for time course by replacing signal increases with this initial euglycemic glucose concentration and by using the final glucose concentration obtained by extrapolating to the corresponding final plasma glucose concentration from Gruetter et al. (1992*a*). The resulting constants were K_t = 3.90 ± 0.82 m*M* (mean ± SD), a maximal transport rate of T_{max} = 1.16 ± 0.29 μmol g^{-1} min^{-1}, and glucose consumption rate of CMR_{glc} = 0.35 ± 0.10 μmol/g (row 2 in Table 1).

(Model A1-A3) The effect of assuming different euglycemic glucose concentrations on T_{max} and K_t was judged by varying $G^{(i)}_{brain}$ within the 95% confidence interval (rows 3–5 in Table 1), i.e., between 0.8 and 1.2 m*M*, within which K_t varied by $\delta K_t = 1.5 \times \delta G^{(i)}_{brain}$ and T_{max} by $\delta T_{max} = 0.45 \times \delta G^{(i)}_{brain}$. These variations are within the experimental error.

In order to evaluate the possibility that intracellular glucose is 0 (G_i = 0), two cases were solved:

Model B: Fast exchange between plasma and extracellular glucose. The assumption that intracellular glucose is 0 (G_i = 0) (see methods) results in

TABLE 1. *Summary of performed numerical analyses of the time courses*

	V_{blood} (%)[a]	V_d (ml/g)	K_t (mM)	T_{max} (μmol/g/min)	CMR_{glc} (μmol/g/min)
(A) fit to % increase in G_i (eq. 5)	3.5	0.77	4.8 ± 2.4	0.80 ± 0.45	0.32 ± 0.16
(A) G_i = 1 m*M* at euglycemia (eq. 4)	3.5	0.77	3.90 ± 0.82	1.16 ± 0.29	0.35 ± 0.10
(A1) G_i = 0.8 m*M* (Eq. 4)	3.5	0.77	3.80 ± 0.76	0.96 ± 0.09	0.30
(A2) G_i = 1 m*M* (Eq. 4)	3.5	0.77	3.60 ± 0.89	1.04 ± 0.11	0.30
(A3) G_i = 1.2 m*M* (Eq. 4)	3.5	0.77	3.20 ± 0.76	1.14 ± 0.15	0.30
Fitting V_{blood} (Eq. 5)	7.0 ± 3.5	0.77	3.90 ± 0.96	1.14 ± 0.15	0.30
Variable V_d (Eq. 4)	3.5	0.81 ± 0.09[b]	3.5 ± 0.91	1.11 ± 0.25	0.35

Values are given as mean ± SD if fitted, fixed parameters are indicated without error. In order to maintain computational efficiency, n ≤3 variables fitted to the data.

[a] Equivalent to ml/100g.

[b] The fit was performed constrained, i.e., in one study, V_d was set to its maximum, 0.965 ml/g.

glucose time courses that parallel the plasma time course closely in the case of free diffusion (solid line in Fig. 5B). This observation is consistent with the estimation that with an average cerebral blood flow of 0.5 ml/g min the glucose influx into the human brain is 2.5 μmol g^{-1} min^{-1}, for an increase from 5 to 10 m*M* plasma concentration, which exceeds the reported change in glucose concentration (Gruetter et al., 1992*a*).

Model C: Michaelis–Menten kinetics for fast exchange at the BBB. When all the glucose is assumed to be confined to the extracellular space (~0.2 ml/g), glucose concentrations that we reported by ^{13}C] NMR (Gruetter et al., 1992*a*; Gruetter et al., 1993) resulted in a $T_{max}/CMR_{glc} > 25$ when fitting the Michaelis–Menten model with $V_d = V_e = 0.2$ ml/g (not shown). Assuming $G_i = 0$ and Michaelis–Menten kinetics at the BBB (Fig. 1C) with $V_d = 0.20$ ml/g, $T_{max}/CMR_{glc} = 25$ or (virtually any range of T_{max}/CMR_{glc}) gave time courses that closely paralleled plasma glucose as illustrated by the dashed line in Fig. 5B.

The measured time courses, however, contained only a very small fraction of the signal that parallels the plasma glucose, as shown by fitting V_{blood} instead of CMR_{glc} (row 6 in Table 1), which is consistent with only a small signal fraction being from the blood compartment.

Calculation of the distribution space of glucose. Since models B and C, which assumed a small distribution space of glucose, are *inconsistent* with the lag in brain glucose observed, V_d in Eq. 1 was also fitted as follows:

We fitted V_d to the time courses, assuming concentrations based on the previous quantification (as in model A) and setting $V_{blood} = 0.035$ ml/g and $CMR_{glc} = 0.35$ μmol g^{-1} min^{-1} (based on previous measurements of this region of the brain) (Heiss et al., 1984; Tyler et al., 1988). The result of this calculation was $K_t = 3.5 \pm 0.9$ m*M* (mean ± SD), $T_{max} = 1.11 \pm 0.25$ μmol g^{-1} min^{-1}, and $V_d = 0.77 \pm 0.01$ ml/g (n = 4). In one study, V_d was 2.1 ml/g, which is above the physical upper limit of 0.965 ml/g. Using, for that study, $V_d = 0.965$ ml/g gave an average $V_d = 0.81 \pm 0.09$ ml/g (n = 5, row 7 in Table 1), which is within the experimental error identical to the distribution space of water, i.e., 0.77 ml/g.

DISCUSSION

Previous measurements of steady-state human cerebral glucose concentrations by ^{13}C NMR gave a concentration of 1 μmol/ml brian volume at euglycemic (4.8 m*M*) plasma concentration (Gruetter et al., 1992*a*). This direct brain glucose measurement was also consistent with all of the brain glucose being in extracellular space, which comprises ~20% of total brain volume (Lund-Andersen, 1979) at a concentration equal to that of plasma glucose. In that extreme case, glucose concentration in the brain cells would be close to zero and transport across the brain cell membranes would be rate-limiting for phosphorylation of glucose. Such a situation is consistent with the observation of saturation kinetics for 2-deoxyglucose transport in brain slices (Bachelard, 1971). Later evidence, however, argued in favor of a very rapid equilibration of glucose in the aqueous phase of *animal* brain based on diffusion measurements of glucose analogs (Lund-Andersen, 1979), distribution volumes of glucose (Holden et al., 1991), and glucose analogs (Gjedde and Diemer, 1983), suggesting that the BBB is rate-limiting for glucose transport, but not phosphorylation. In addition, previous direct ^{13}C NMR measurements of total *rat* brain glucose concentration (Mason et al., 1992) are similar to very recent measurements of extracellular glucose concentration using microelectrodes (Silver and Erecinska, 1994) suggesting that concentrations of intra- and extracellular brain glucose are similar in *rat* brain. The present results argue in favor of a similar situation

in the *human* brain in vivo under normal physiologic conditions, since this study demonstrates a significantly delayed rise in brain glucose relative to plasma glucose, indicating saturation kinetics and a large physical distribution space of glucose in human brain (row 7 in Table 1).

The parameters for glucose transport obtained from the time courses of plasma glucose increments (row 1 in Table 1) are similar to those reported previously from the relationship of plasma glucose versus brain glucose at steady-state (Gruetter et al., 1992*a*). Both approaches used the symmetric Michaelis–Menten model for glucose transport across the BBB to calculate the kinetic constants. The kinetic parameters of steady-state glucose transport obtained by ^{13}C NMR spectroscopy predict the time course of brain glucose increments accurately, as illustrated in Fig. 5A, further emphasizing the consistency of the experimental evidence. Comparison of this study with previous measurements of brain glucose transport in humans using radioisotope methods (Table 2) shows that the K_t values are highly consistent among the different methods used and falls slightly below the normal fasting glucose concentration. However, as shown in Table 2, T_{max} values obtained by radioisotope methods scatter by a fivefold range. Euglycemic brain glucose concentrations calculated from the symmetric transport model (Eq. 3), using the respective kinetic constants given in columns 4 and 5 in Table 2 and the accepted standard of 0.3 μmol g^{-1} min^{-1} for CMR_{glc} for gray matter (Heiss et al., 1984; Tyler et al., 1988), range thus from −0.6 to 2 μmol/g (column 6 in Table 2), with none of the previous studies being consistent with the NMR measurement (row 5 in Table 2). This discrepancy becomes more apparent when comparing direct in vivo NMR quantification at 10 m*M* plasma glucose concentration with predicted values from isotope measurements (column 7 in Table 2): Three of the four PET studies predict glucose concentrations below the euglycemic NMR value. If the K_m for hexokinase is assumed to be on the order of 50 μ*M*, then it is clear that the brain glucose concentrations derived from these studies predict that brain glucose transport is rate-limiting for metabolism at euglycemia in contrast to the conclusion of the present report.

It is well established that glucose transport is mediated by glucose transporters, which are a homologous class of transmembrane proteins with transporter-type and species-specific differences (Mueckler, 1994). Most of the present evidence suggests that the erythrocyte/liver type glucose transporter, GLUT-1, is the abundant transporter molecule at the membranes of the endothelial cells comprising the BBB (Pardridge et al., 1990). A different, recently identified, brain-type glucose transporter, GLUT-3, (Gerhart et al., 1992) seems to be distributed mainly within brain tissue that has little measurable GLUT-1 (Maher et al., 1993; Mantych et al., 1992). The evidence we obtained suggests that the BBB is the major rate-limiting step for glucose entry into human brain, with an overall higher transport capacity at the intracellular/extracellular interface compared to that at the BBB. Even though transport rates within the brain might be extremely high, leading to a single, well-mixed brain glucose pool, the transport rate will be limited by the slowest step of the multiple sequential transport steps, which we propose in the human brain to be at the BBB.

We have obtained ^1H NMR spectra of glucose from the brain of healthy volunteers by taking the difference between spectra obtained at euglycemia and during a glucose infusion. Since these difference spectra contain only signals from glucose, the high sensitivity of ^1H NMR allowed measurement of changes in glucose levels with 3-min time resolution. The noninvasive, time-resolved measure-

TABLE 2. *Michaelis-Menten constants of blood-brain glucose transport in humans*

Citation	Method	No. of subjects	K_t (m*M*)	T_{max} (μmol/g^{-1} min^{-1})	G_{brain} [a] (μmol/g)	G_{brain} [b] (μmol/g)
Brooks et al. (1986)	PET	4	4.2	0.4	−0.6[c]	−0.1[c]
Feinendegen et al. (1986)	PET	6	3.8	2.0	2.0	4.1
Gutniak et al. (1990)[d]	PET	8	4.1	0.5	−0.2[c]	0.4
Blomqvist et al. (1991)	PET	8	4.1	0.6	0.1	0.8
Gruetter et al. (1992*a*)	MR	7	4.8	1.1	1.0 ± 0.1[e]	2.4 ± 0.2[e]

[a] Brain glucose concentrations were calculated at a plasma glucose concentration of 4.8 m*M* from the given transport constants using Eq. 3 and assuming a CMR_{glc} of 0.3 μmol/g^{-1} min^{-1} (Heiss et al., 1984).

[b] Derived at a plasma glucose of 10 m*M* as in footnote [a].

[c] Constants from this study are inconsistent with a positive brain glucose concentration at euglycemia.

[d] Derived by fitting $k_1 = T_{max}/(K_t + G_{plasma})$ to k_1 measured at two different G_{plasma}.

[e] Brain glucose concentration was measured directly in this study.

ment of brain glucose changes from small volumes by ^{1}H NMR opens the prospect of measuring glucose transport and rates of glycolysis noninvasively; decreases in brain glucose concentrations have been reported using ^{1}H NMR during brain visual activation (Merboldt et al., 1992; Chen et al., 1993). Observations of the (resolved) $^{\alpha}H1$ resonance at 5.23 ppm, as indicated in the difference spectrum (Fig. 2B), may become a routine method to quantify cerebral glucose, particularly at hyperglycemia. Alternatively, it has been shown in cat brain that measurement of the H1 proton coupled to the C1 carbon can be measured during [1-^{13}C] glucose infusions, when using strong gradients and multiple-quantum coherence to eliminate the water signal, with a sensitivity that may be sufficient to measure glucose influx rates and spatial distribution during hyperglycemia (van Zijl et al., 1992; Inubushi et al., 1993; van Zijl et al., 1993). Using either method, from the subsequent difference spectra it may, thus, be possible to deduce cerebral glucose concentrations at lower plasma glucose concentrations. Simulations based on the ^{13}C NMR quantification of cerebral glucose indicate that measurement of the cerebral glucose *concentration* considerably improves the accuracy of the determination of transport kinetics.

Conclusions

This study confirms our earlier observations that difference ^{1}H spectroscopy is a useful tool to investigate glucose transport in the human brain since these difference spectra contain only intensity from glucose. As such, NMR is to date the only method that permits noninvasive measurement of cerebral glucose in human brain under physiological conditions.

The direct measurement of glucose concentration and, potentially, transport and metabolism by ^{1}H NMR spectroscopy adds to existing measurements of PET, indicator-dilution, and other techniques since it does not use ionizing radiation and is less invasive. Hence, NMR may be a useful and cost-effective alternative to PET for certain studies such as longitudinal and pediatric studies.

The time course of the brain glucose difference is consistent with the previous determination of BBB transport kinetics by ^{13}C NMR in *humans* (Gruetter et al., 1992a). The large distribution space derived from the present study indicates that intracellular and extracellular glucose levels are similar in the human brain. The implied rapid transport rates within the brain suggest that transport across the BBB is the rate-limiting step of the multiple steps involved in glucose *transport*. Demonstration of a significant brain glucose concentration is direct experimental evidence that glucose transport is not rate-limiting for metabolism, which suggests that glucose transport does not regulate human brain glucose metabolism.

Acknowledgment: Supported by U.S. Public Health Service grants NS28790 and DK34576 from the National Institutes of Health, Bethesda, MD, U.S.A. and by a grant from the Juvenile Diabetes Foundation (E.J.N.).

REFERENCES

Bachelard HS (1971) Specificity and kinetic properties of monosaccharide uptake into guinea pig cerebral cortex *in vitro*. *J Neurochem* 18:213–222

Baum J, Tycko R, Pines A (1985) Broadband and adiabatic inversion of a two-level system by phase-modulated pulses. *Phys Rev A* 32:3435–3447

Blondet P, Decorps M, Confort S, Albrand JP (1987) ^{1}H In vivo NMR spectroscopy with surface coils. Hard pulse water suppression sequences and spatial localization. *J Magn Reson* 75:434–451

Blomqvist G, Gjedde A, Gutniak M, Grill V, Widén L, Stone-Elander S, Hellstrand E, (1991) Facilitated transport of glucose from blood to brain in man and the effect of moderate hypoglycemia on cerebral glucose utilization. *Eur J Nucl Med* 18:834–837

Brooks DJ, Gibbs JSR, Sharp P, Herold S, Turton DR, Lthra SK, Kohner EM, Bloom SR, Jones T (1986) Regional Cerebral glucose transport in insulin-dependent diabetic patients studied using [^{11}C]3-*O*-methyl-D-glucose and positron emission tomography. *J Cereb Blood Flow Metab* 6:240–244

Carruthers A (1990) Facilitated diffusion of glucose. *Physiol Rev* 70:1135–1176

Chen W, Ackerman JJH (1989) Surface coil single-pulse localization in vivo via inhomogenous surface spoiling magnetic gradient. *NMR Biomed* 1:205–207

Chen W, Novotny EJN, Zhu XH, Rothman DL, Shulman RG (1993) Localized ^{1}H NMR measurement of glucose consumption in the human brain during visual stimulation. *Proc Natl Acad Sci U S A* 90:9896–9900

Connelly A, Counsell C, Lohman JAB, Ordidge RJ (1988) Outer volume suppressed image related in vivo spectroscopy (OSIRIS), a high-sensitivity localization technique. *J Magn Reson* 78:519–525

Crone C (1965) Facilitated transfer of glucose from blood into brain tissue. *J Physiol* 181:103–113

De Fronzo R, Tobin JD, Andres R (1979) Glucose clamp technique: A method of quantifying insulin secretion and resistance. *Am J Physiol* 237:E214–223

DeVivo DC, Trifiletti RR, Jacobson RI, Ronen GM, Behmand RA, Harik SI (1991) Defective glucose transport across the blood-brain barrier as a cause of persistent hypoglycorrhachia, seizures, and developmental delay. *N Engl J Med* 325:703–709

Feinendegen LE, Herzog H, Wieler H, Patton DD, Schmid A (1986) Glucose transport and utilization in the human brain: Model using carbon-11 methylglucose and positron emission tomography. *J Nucl Med* 27:1867–1877

Gerhart DZ, Broderius MA, Borson ND, Drewes LR (1992) Neurons and microvessels express the brain glucose transporter protein GLUT3. *Proc Natl Acad Sci U S A* 89:733–737

Gjedde A (1982) Calculation of Cerebral Glucose Phosphorylation from brain uptake of glucose analogs in vivo: A re-examination. *Brain Res Rev* 4:237–274

Gjedde A, Diemer NH (1983) Autoradiographic determination of regional brain glucose content. *J Cereb Blood Flow Metab* 3:303–310

Gjedde A (1992) Blood-brain glucose transfer. In: *Handbook of Experimental Pharmacology, Vol. 103: Physiology and Pharmacology of the Blood-Brain Barrier* (Bradbury MWB, ed), New York, Berlin, Springer Verlag, pp 65–117

Gjedde A, Christensen O (1984) Estimates of Michaelis–Menten constants for the two membranes of the brain endothelium. *J Cereb Blood Flow Metabol* 4:241–249

Gruetter R (1993) Automatic, localized in vivo adjustment of all first- and second-order shim coils. *Magn Reson Med* 29:804–811

Gruetter R, Novotny EJ, Boulware SD, Rothman DL, Mason GF, Shulman GI, Shulman RG, Tamborlane WV (1992*a*) Direct measurement of brain glucose concentrations in humans by ^{13}C] NMR spectroscopy, *Proc Natl Acad Sci U S A* 89:1109–1112 (Erratum appears in vol. 89:12208)

Gruetter R, Novotny EJ, Boulware SD, Rothman DL, Mason GF, Shulman GI, RG Shulman, Tamborlane WV (1993) Non-invasive measurements of the cerebral steady-state glucose concentration and transport in humans by ^{13}C magnetic resonance. In: *Frontiers in Cerebral Vascular Biology: Transport and its Regulation* (Drewes LR, Betz AL, eds) *Adv Exp Med Biol 331*, New York Plenum Press, pp 35–40

Gruetter R, Novotny EJ, Boulware SD, Mason GF, Rothman DL, Prichard JW, Shulman RG (1994) Localized ^{13}C] NMR spectroscopy in the human brain of amino acid labeling from D-[1-^{13}C]glucose. *J Neurochem* 63:1377–1385

Gruetter R, Rothman DL, Novotny EJ, Shulman GI, Prichard JW, Shulman RG (1991) Detection of Glucose by ^1H NMR spectroscopy of the human brain during acute hyperglycemia. *10th Annual Meeting, Society of Magnetic Resonance in Medicine, Works-in-Progress*, p. 1014, San Francisco, August 10–16

Gruetter R, Rothman DL, Novotny EJ, Shulman GI, Prichard JW, Shulman RG (1992*b*) Detection and Assignment of the glucose signal in ^1H NMR difference spectra of the human brain. *Magn Reson Med* 27:183–188

Gutniak M, Blomqvist G, Widen L, Stone-Elander S, Hamberger B, Grill V (1990) D-[U-^{11}C]glucose uptake and metabolism in the brain of insulin-dependent diabetic subjects. *Am J Physiol* 258:E805–E812

Gyngell MS, Michaelis T, Hörstermann D, Bruhn H, Hänicke W, Merboldt KD, Frahm J (1991) Cerebral glucose is detectable by localized proton NMR spectroscopy in normal rat brain in vivo. *Magn Reson Med* 19:489–495

Hino A, Ueda S, Mizukawa N, Imahori Y, Tenjin H (1992) Effect of hemodilution on cerebral hemodynamics and oxygen metabolism. *Stroke* 23:423–426

Heiss WD, Pawlik, Herholz K, Wagner R, Göldner H, Wienhard K (1984) Regional kinetic constants and cerebral metabolic rate for glucose in normal human volunteers determined by dynamic positron emission tomography of [^{18}F]-2-fluoro-deoxy-D-glucose. *J Cereb Blood Flow Metabol* 4:212–223

Holden JE, Mori K, Dienel GA, Cruz NF, Nelson T, Sokoloff L (1991) Modeling the dependence of hexose distribution volumes in brain on plasma glucose concentration: Implications for estimation of the local 2-deoxyglucose lumped constant. *J Cereb Blood Flow Metab* 11:171–182

Inubushi T, Morikawa S, Kito K, Arai T (1993) ^1H-detected in vivo ^{13}C NMR spectroscopy and imaging at 2T magnetic field: Efficient monitoring of ^{13}C-labeled metabolites in the rat brain derived from [1-^{13}C]glucose. *Biochem Biophys Res Commun* 191:866–72

Kalaria RN, Gravina SA, Schmidley JW, Perry G, Harik SI (1988) The glucose transporter of the human brain and blood-brain barrier. *Ann Neurol* 24:757–764

Kalaria RN, Harik SI (1989) Reduced glucose transporter at the blood-brain barrier and in cerebral cortex in Alzheimer's disease. *J Neurochem* 53:1083–1088

Kreis R, Ross BD (1992) Cerebral metabolic disturbances in patients with subacute and chronic diabetes mellitus: Detection with proton MR spectroscopy. *Radiology* 184:123–130

Levitt MH, Ernst RR (1983) Composite pulses constructed by a recursive expansion procedure. *J Magn Reson* 55:247–254

Lund-Andersen H (1979) Transport of glucose from blood to brain. *Physiol Rev* 59:305–352

Maher F, Vannucci SJ, Simpson IA (1993) Glucose transporter isoforms in brain: Absence of GLUT3 from the blood-brain barrier. *J Cereb Blood Flow Metab* 13:342–345

Mahler HR, Cordes EH (1971) *Biological Chemistry, 2nd ed.* Harper & Row: New York, pp 275–294

Mantych GJ, James DE, Chung HD, Devaskar SU (1992) Cellular localization and characterization of GLUT3 glucose transporter isoform in human brain. *Endocrinology* 131:1270–1278

Marchal G, Rioux P, Petit-Taboué MC, Sette G, Travère JM, Le Poec C, Courtheoux P, Derlon JD, Baron JC (1992) Regional cerebral oxygen consumption, blood flow, and blood volume in healthy human aging. *Arch Neurol* 49:1013–1020

Mason GF, Behar KL, Rothman DL, Shulman RG (1992) NMR determination of intracerebral glucose concentration and transport kinetics in rat brain. *J Cereb Blood Flow Metabol* 12:448–455

Mason GF, Gruetter R, Rothman DL, Behar KL, Shulman RG, Novotny EJ (1995) Simultaneous determination of the rates of the TCA cycle, glucose utilization, alpha-ketoglutarate/glutamate exchange, and glutamine synthesis in human brain by NMR. *J Cereb Blood Flow Metab* 15:12–25

Merboldt KD, Bruhn H, Hänicke W, Michaelis T, Frahm J (1992) Decrease of glucose in the human visual cortex during photic stimulation. *Magn Reson Med* 25:187–194

Michaelis T, Merboldt KD, Hänicke W, Gyngell ML, Frahm J (1991) On the identification of cerebral metabolites in localized ^1H NMR spectra of human brain in vivo. *NMR Biomed* 5:90–98

Mueckler M, Caruso C, Baldwin SA, Panico M, Blench I, Morris HR, Allard WJ, Lienhard GE, Lodish HF (1985) Sequence and structure of a human glucose transporter. *Science* 229:941–945

Mueckler M (1994) Facilitative glucose transporters. *Eur J Biochem* 219:713–725

Novotny EJ, Gruello R, Rothman DL, Boulware SD, Shulman RG (1992) ^1H NMR studies of glucose transport in the human brain. 11th Annual Meeting Society of Magnetic Resonance in Medicine, Berlin, August 8–14, p. 1961

Novotny EJ, Gruetter R, Rothman DL, Boulware SD, Tamborlane WV, Shulman RG (1993) Chronic hyperglycemia does not alter steady-state human brain glucose concentrations: A ^{13}C NMR study. *12th Annual Meeting, Society of Magnetic Resonance in Medicine* New York, August 14–20, p 324

Ordidge RJ, Connelly A, Lohman JAB (1986) Image-selected in vivo spectroscopy (ISIS). A new technique for spatially selective NMR spectroscopy. *J Magn Reson* 66:283–294

Pappenheimer JR, Setchell BP (1973) Cerebral glucose transport and oxygen consumption in sheep and rabbits. *J Physiol* 283:529–551

Pardridge WM (1983) Brain metabolism: A perspective from the blood-brain barrier. *Physiol Rev* 63:1481–1535

Pardridge WM, Boado RJ, Farrell CR (1990) Brain-type glucose transporter (GLUT-1) is selectively localized to the blood-brain barrier. *J Biol Chem* 265:18035–18040

Pelligrino DA, LaManna JC, Duckrow RB, Bryan RM, Jr, Harik SI (1992) Hyperglycemia and blood-brain barrier glucose transport. *J Cereb Blood Flow Metab* 12:887–899

Petroff OAC, Spencer DD, Alger JR, Prichard JW (1989) High-field proton magnetic resonance spectroscopy of human cerebrum obtained during surgery for epilepsy. *Neurology* 39:1197–1202

Press WH, Flannery BP, Teukolsky SA, Vetterling WT (1989) *Numerical Recipes in Pascal.* Cambridge University Press, Cambridge, England, pp 617–623

Raichle ME (1983) Circulatory and metabolic correlates of brain function in normal humans. In: *Handbook of Physiology: The nervous System V*, Williams & Wilkins, Baltimore, MD, pp. 643–674

Sabatini U, Celsis P, Viallard G, Rascol A, Marc-Vergnes JP (1991) Quantitative assessment of cerebral blood volume by

single-photon emission computed tomography. *Stroke* 22:324–330

Shaka AJ, Freeman R (1985) Spatially selective pulse sequences: Elimination of harmonic responses. *J Magn Reson* 62:340–345

Shulman GI, Rothman DL, Jue T, Stein P, DeFronzo RA, Shulman RG (1990) Quantitation of muscle glycogen synthesis in normal subjects and subjects with non-insulin-dependent diabetes by ^{13}C nuclear magnetic resonance spectroscopy. *N Engl J Med* 322:223–228

Siesjö BK (1978) *Brain Energy Metabolism*. New York, John Wiley & Sons Ltd, pp 110–117

Silver IA, Erecinska M (1994) Extracellular glucose concentration in mammalian brain: Continuous monitoring of changes during increased neuronal activity and upon limitation in oxygen supply during normo-, hypo- and hyperglycemic animals. *J Neurosci* 14:5068–5076

Sokoloff L (1984) Modeling metabolic processes in the brain in vivo. *Ann Neurol* 15:S1–S11

Stewart MA, Sherman WR, Kurien MM, Moonsammy GI, Wisgerhof M (1967) Polyol accumulations in nervous tissue of rats with experimental diabetes and galactosaemia. *J Neurochem* 14:1057–1066

Silver MS, Joseph RI, Hoult DI (1984) Highly selective $\pi/2$ and π pulse generation. *J Magn Reson* 59:347–351

Tyler JL, Strother SC, Zatorre RJ, Alivisatos B, Worsley KJ, Diksic M, Yamamoto YL (1988) Stability of regional cerebral glucose metabolism in the normal human brain measured by positron emission tomography. *J Nucl Med* 29:631–642

van Zijl PCM, Moonen CTW, Davies D, DesPres D, Andersen L, Parker R (1992) Direct monitoring of glucose transport in the brain. *11th Annual Meeting, Society of Magnetic Resonance in Medicine* Berlin, August 6–12:Abstract 550

van Zijl PCM, Chesnick AS, DesPres D, Moonen CTW, Ruiz-Cabello J, van Gelderen P (1993) In vivo proton spectroscopy and spectroscopic imaging of [1-^{13}C]-glucose and its metabolic products. *Magn Reson Med* 30:544–551